Permittivity and Loss Characterization of Polymer Films for Terahertz Applications

Tsz ki Liu

Department of Electrial Engineering, City University of HongKong, HongKong, China

ken117702@gmail.com

Abstract. With the development of science, terahertz (THz) technology has matured gradually. More attention has been given to THz technology in recent years due to its superiority for non-destructive testing. Dielectric polymers are widely used in electrical engineering because of their unique electrical properties. Spectral detection plays a vital role in studying the internal motion and micro-scale forces. THz time-domain spectroscopy (THz-TDS) is a powerful complement to other spectroscopy techniques because of its unique frequency band that energetically vibrates and rotates the polymer structure. Herein, we apply THz-TDS with an effective frequency of 0.1–1 THz at 55% relative humidity. TDS at 0.1–1 THz to conduct fundamental research on several commonly utilized dielectric non-polar and polar polymer films including PC, FTPE, PMMA, HDPE, PA6, PET, PP. In this study, the THz complex refractive index and dielectric constants of various polymer films are determined and compared with previously reported values. In addition, the loss mechanism of THz radiation in polymers is characterized by correlating the absorption coefficients of the materials with the loss tangents. Herein, we demonstrate that the sample preparation significantly impacts the loss behavior of polymer materials and quantify the effect of crosslinking on the dielectric constant across the entire frequency band. The findings presented herein are expected to contribute to the design and development of optical and electronic devices in the future.

Keywords: Terahertz Applications; Polymer Films; Dielectric Constant.

1. Research Background of the Topic

Terahertz (THz) waves are electromagnetic radiation in the band between microwave and infrared wave [1] as shown in Figure 1. However, this particular band cannot be thoroughly studied using either optical or microwave theories. Before the 1980s, few techniques were available for rapid and accurate generation and detection of THz waves, which severely limited their application. More recently, with the steady maturation of femtosecond lasers, photoconductive switches, and optical rectification technology, THz physics has been more widely studied. In the 10 past years, solid-state electronics based on optoelectronic semiconductors have proven useful for the excitation and generation of THz waves. This was a breakthrough for THz research and led to a dramatic increase in the utilization of THz technology [2].

2. Background

2.1 Research Background of the Topic

Terahertz (THz) waves are electromagnetic radiation in the band between microwave and infrared wave [1] as shown in Figure 1. However, this particular band cannot be thoroughly studied using either optical or microwave theories. Before the 1980s, few techniques were available for rapid and accurate generation and detection of THz waves, which severely limited their application. More recently, with the steady maturation of femtosecond lasers, photoconductive switches, and optical rectification technology, THz physics has been more widely studied. In the 10 past years, solid-state electronics based on optoelectronic semiconductors have proven useful for the excitation and generation of THz waves. This was a breakthrough for THz research and led to a dramatic increase in the utilization of THz technology [2].

Before extracting the signal characteristics containing the sample information from the THz time-domain waveform, a Fourier transform is applied to the raw signal, converting it from the time domain to the frequency domain. The frequency-domain signal is then analyzed to derive the refractive index, absorption coefficient, and related physical and chemical parameters such as the extinction coefficient. The acquisition of the optical parameters does not rely on a K–K relationship, which is a unique advantage of THz-TDS technology and is not possible with any other optical or microwave technology currently available.

When T > 1 T, water molecules are polar and strongly absorb THz waves. Therefore, to eliminate the influence of the water vapor in the air on the THz-TDS measurements [3], the light path through which THz electromagnetic radiation passes should be sealed, evacuated, and filled nitrogen to exclude any water vapor.

2.2 Polymer Samples

The thickness of each polymer sample to be studied was measured by a high-precision digital external micrometer that adjusts easily (Figure 1). The results (Table 1) show that the polymer specimens had a range of thicknesses. The samples were not too thin (above 0.5 mm) so that the measurement result would be significantly affected by the interference or too thick (below 4mm) so that the measured THz signal would be weak.



Figure 1. Digital micrometer

Table 1. Thicknesses of polymer samples

Polymer	measured Thickness (mm)
PMMA(1mm)	0.884
PVC(0.5mm)	0.422
HDPE(3mm)	3.188
PTFE(0.5mm)	0.46
PC(0.5mm)	0.512
PP(0.5mm)	0.408
PET(0.5mm)	0.464
ABS(2mm)	2.019
PA6(1mm)	1.016

2.3 Data Acquisition and Processing

Before the experiment, an ultrafast laser laboratory ventilation system was initiated to cool the room to 22 °C and reduce the humidity to less than 80% RH. Before measuring, the laser was run for a few minutes to allow the light output power to stabilize. The femtosecond pump source was then turned on, and the time constant was set to 100 ms, the sensitivity was set to 100 mV, and the dynamic range was set to 24 dB. The femtosecond pump source is shown in fig 6.A high-voltage power supply was then connected to the pump source and set to the working state; the output voltage was set at 40 V, and the modulation frequency was 31.5 KHz. The translation platform, acquisition card, and other equipment were checked before experimentation. The translation platform step distance was set to 2.5 mm with a step speed of 5 m/s. Before each experiment, a measurement of air only (no sample) was conducted to confirm that there was no problem with the system.

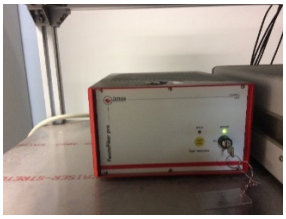


Figure 2. Pump source power

The prepared thin-film sample was placed for testing such that the THz wave is vertically incident to the sample showing in fig 7. The height of the sample rack was fixed so that the THz wave can pass through the sample completely. TerHz control software was used to execute the data collection and storage. The micro-signals produced in the experiment were amplified by the phase-locked amplifier then collected synchronously by the computer control program. Finally, the THz wave time-domain signals are displayed and stored on the computer for further processing.

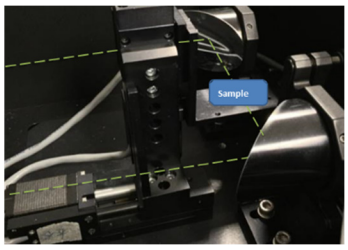


Figure 3. Position of sample

2.4 Data Processing

The factors influencing the accuracy of the experimental results are as follows. The first factor is the accuracy of the measurement data, which is strongly influenced by the SNR of the system. The SNR may be affected by the instability of the femtosecond laser output, the noise of the detector, the error in the delay line step, and the noise generated by the gas disturbance. Measurement error may also result from the transmission of the THz through water vapor. Further, FFT transformation accuracy influences the accuracy of the final result [4]. In the process of data collection, the influence of these aspects should be eliminated or reduced as much as possible.

TerHz software stores the measured data in CSV format. These data are then processed using MATLAB to obtain the time-domain data of the reference signal and sample signal. In order to reduce the measurement error in the data, each test was repeated three times to obtain a group of replicates; the signals were then added in the time domain and subsequently divided by the number of measurements (because the time interval and time point of the THz time-domain waveform are consistent between measurements).

At this stage, the mean value needs to be pre-processed before the Fourier transform is applied. The first step is to subtract the mean value: after averaging the amplitude of each time point in the whole-time domain, the corresponding direct flow is calculated and the dc component is removed. The calculated spectrum is limited to the discrete points of the spectrum (i.e., it is not a continuous-frequency function); this phenomenon is called the fence effect in digital signal processing. To avoid this issue, under the premise of not changing the time domain data, a zero-value point is appended at the end of the data series such that the spectral lines in the frequency domain become denser. However, the zeroing does not change the resolution of the spectrum. After these pre-processing steps, the Fourier transformation is performed. The spectrum range after the Fourier transformation is determined by the dynamic range of the system.

Finally, the refractive index and absorption coefficient are calculated. This involves obtaining the transmission function from the frequency-domain signal, $T(\omega)$, which comprises an amplitude spectrum, $\rho(\omega)$, and phase spectrum, $\phi(\omega)$. Given the sample thickness, d, the known quantities

are substituted into Eqs. 33 and 35 to calculate the refractive index and absorption coefficient. Hence, other transmission rates, power spectra, and various parameters can be calculated.

Although the liquid structure of water molecules is difficult to measure and characterize directly, the structure and kinetics of isolated water clusters provide a basis to quantitatively study the intermolecular forces and hydrogen bond arrangements [5]. The interaction between water molecules via hydrogen bonds forms a complex multi-body system in which water molecules rotate or vibrate near equilibrium positions. The relaxation time of this type of motion is generally on the order of picoseconds and sub-picoseconds. Therefore, water will exhibit positive absorption of THz waves [6,7].

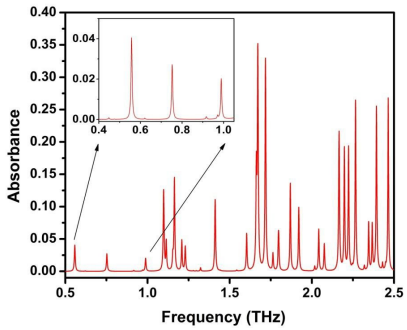


Figure 4. Absorbance spectrum of water vapor (inset: first three peaks enlarged)

Martin et al. [8] characterized the THz spectrum of water vapor in 1989, reporting that water vapor exhibits nine absorption peaks in the THz band. However, in 1998, Alan Cheville et al. [9] reported conflicting results. Takashi et al. [10] reported the THz spectrum of water with no absorption peaks in the 0–1.4 THz range. Wei Shi et al. [11] measured the THz spectrum (0.2–4.2 THz) of water and water vapor in 2004 using a more reliable THz source and revealed that water vapor exhibits 27 resonance absorption peaks in this range. Figure 4 shows the absorption spectrum of water vapor in the range of 0.5–2.5 THz [12]. For better visualization, the first three peaks (located at 0.558, 0.753, and 0.996 THz) are magnified in the inset.

In this experiment, there are potential sources of water that may influence the results: the water vapor in the air if the relative humidity fluctuates from the control value and the water contained in the sample itself.

3. Undamental Results

3.1 Terahertz Time-domain Spectral Analysis of Typical Polymers

THz-TDS was performed on the polymer specimens with thicknesses ranging from 0.5 to 3 mm. THz encapsulation should be optimized with low dielectric constant and low loss materials, so several non-polar organic materials were characterized: HDPE, polypropylene PP, and PTFE. In addition, several polar materials were tested: PET, PC, PA6, PMMA, and PVC.

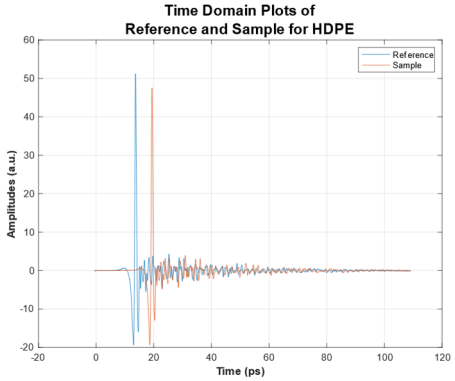


Figure 5. Time domain pulses of the HDPE sample and reference

Figure 5 below shows the time-domain pulses for the HDPE sample and the reference measurement. The delay of the sample pulse was slightly lower (by about 5 ps) than that for the reference pulse; this was due to the refractive index of the sample. Further, the amplitude of the sample pulse was slightly lower than that for the reference pulse; this was attributed to the absorption and dispersion of the signal by the sample.

THz frequency-domain signals contain amplitude and phase information as shown in Figures 5 and 16, respectively, for HDPE. Above 1.5 THz, both the sample and the reference spectra degenerate into high-oscillation noise. The phase diagram (Figure 5) shows the unwrapping phase that is continuously added by adding an additional 2π package at each successive stage. The phase at THz oscillates rapidly, indicating that there are infinitely many solutions for inverting any equation utilizing phase (in contrast, a flat phase angle would mean that the electromagnetic waves do not oscillate). The unwrapping phase only provides a single solution. It should be noted that the phase is negative simply due to the symbolic convention of the propagation direction.

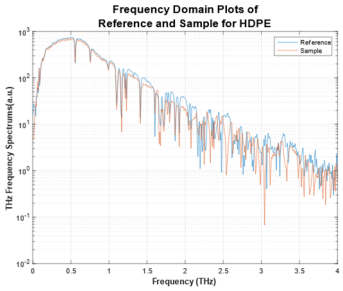


Figure 6. Frequency-domain HDPE and reference spectra

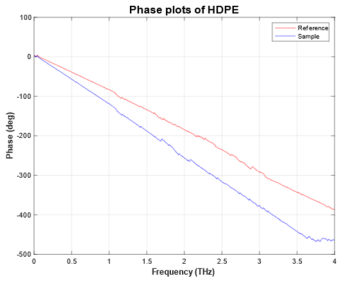


Figure 7. Phases of the HDPE and reference time-domain pulses

Figures 8 and 9 show the variation of the refractive index, n, with the frequency for several polymers. The refractive index of non-polar polymer HDPE was approximately constant at about 1.53 within this frequency range (Figure 5). On the other hand, for some polar polymers, the refractive index decreased with increasing frequency, exhibiting anomalous dispersion properties (Figure 6). The refractive indexes of the non-polar polymers were lower than those of the polar polymers, with that of PTFE being the lowest followed by PP then HDPE. Among the polar polymers, the refractive index of PMMA was the lowest (though still greater than those of the non-polar polymers), whereas that of PA6 was the greatest.

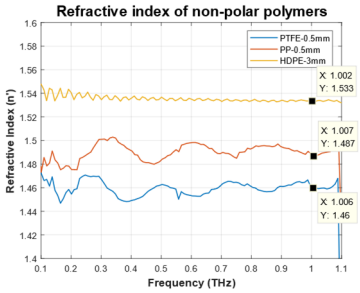


Figure 8. Refractive indexes of non-polar polymers

Because of water absorption and thickness, PP and PTFE exhibited more profound ripples than HDPE.

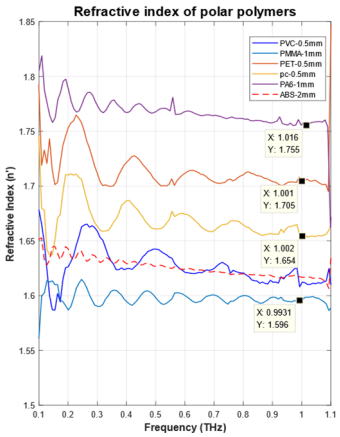


Figure 9. Refractive indexes of polar polymers

The relative dielectric constants ε_r, of these polymers are shown in Figures 10 and 11. These parameters were calculated using the equation $\varepsilon_r = n^2 - k^2$ based on the measured index of refraction and extinction coefficient determined as described above. For the non-polar and polar polymers of dielectric constants is almost agreement from the literature value [13]. The real part of the dielectric constant of HDPE, which is non-polar in some media, remains basically unchanged around 2.3 as the frequency is varied. However, the polar polymers exhibit anomalous dispersion properties in the THz band; this is attributed to the dipole motion with changing frequency due to the damping of the surrounding dielectric material as the orientation polarization cannot fully follow the changes in the electric field.

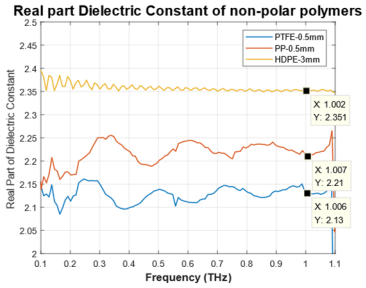


Figure 10. Real parts of the dielectric constants of non-polar polymers

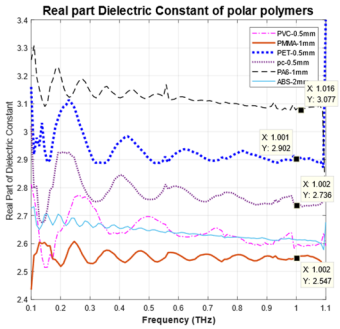


Figure 11. Real part dielectric constant of polar polymers

Figures 12 and 13 show the absorption coefficients, α, of the non-polar and polar polymers as functions of frequency. Among them, HDPE and PTFE absorb very weakly in the THz band; for this

reason, they are often used as base materials for THz measurements in composite systems. Although the C–H bonds in HDPE have a certain bond moment (about 0.3 D, where 1 D = 3.34 × 10^{-34} C·m), the bond moments cancel each other out because of the symmetry of the macromolecular chain; therefore, HDPE has no polarity. Hence, HDPE, PTFE, and PP are considered can be good candidates for Thz optical devices such as lenses and windows due to their slowly varying constant refractive indexes and low absorption coefficients [13].

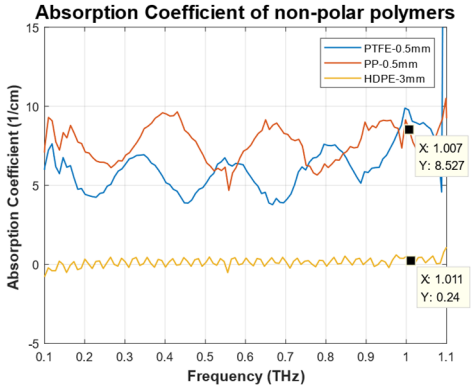


Figure 12. Absorption coefficients of non-polar polymers

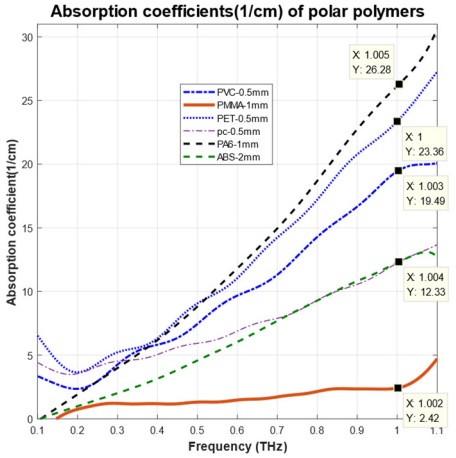


Figure 13. Absorption coefficients of polar polymers

The loss tangent is related to the index of refraction and extinction coefficient according to the equation tan δ = (2nk)/ (n^2 – k^2). Assuming low loss and high organic material loss between standard classification, HDPE, PTFE, and PP are expected to be low loss materials and PP, PC and ABS, and PMMA are expected to exhibit high loss tangents. The loss tangents for non-polar and polar polymers are shown in Figures 14 and 15.

A dielectric in an alternating electric field will consume electric energy and release heat, resulting in dielectric loss. The dielectric loss of PET decreases as the frequency increased due to the action of viscous resistance of the medium, which caused the dipole steering process to lag behind the change in the electric field such that forced movement occurs under the action of the electric field. The other polymers, such as PET, ABS, and PA6, have larger structural units so the polar molecules are unable to keep up with the changes in the electric field in the high-frequency THz electric field. Hence, the amplitude of the orientation polarization decreases with the increase of frequency so the dielectric loss decreases with increasing frequency.

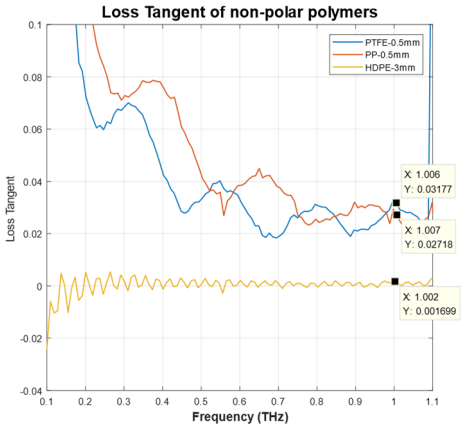


Figure 14. Loss tangents of non-polar polymers

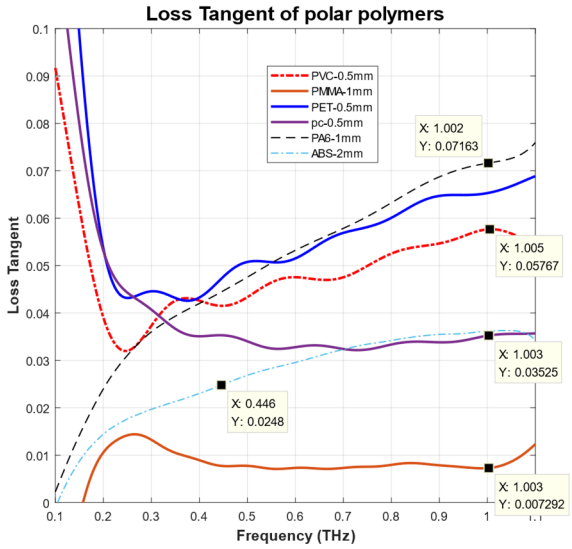


Figure 15. Loss tangents of polar polymers

Table 2. Comparison of measured polymer properties with those that were reported previ

At 1 THz		This study				Previous studies			
Material	Thickness (mm)	n	α (cm-1)	ε_r	tanδ	n [13]	α (cm-1)	ε_r	tanδ
HDPE	3.188	1.533	0.5472	2.351	0.001699	1.534	0.5 [18]	2.37 [15]	0.002 [15]
PTFE	0.46	1.46	8.527	2.135	0.02937	1.445	0.6 [14]	2.06 [16]	0.008 [13]
PP	0.408	1.487	9.885	2.216	0.0324	1.510	0.58 [14]	2.21 [16]	0.008 [13]
PMMA	0.884	1.596	1.306	2.547	0.000389	1.596	11.3 [14]	2.64 [17]	0.06 [13]
PET	0.464	1.705	22.72	2.902	0.06302	1.712	20 [13]	2.98 [16]	0.063 [13]
ABS	2.019	1.617	12.56	2.614	0.037	1.650	17 [13]	2.612 [13]	0.05 [13]
PA6	1.016	1.756	27.41	3.087	0.07649	1.736	26 [13]	3.01 [13]	0.07 [13]
PC	0.512	1.656	13.9	2.736	0.03946	1.651	9.6 [13]	2.612 [13]	0.028 [19]
PVC	0.422	1.612	21.13	2.595	0.06244	/	/	/	/

Table 2 shows the measured parameters for the polymers compared with those reported in the literature; all parameters were extracted at a single frequency of about 1 T. The parameters for some polymers (such as PMMA, PTFE, and PP) exhibited poor accuracy because of wave absorption and sample thickness (0.5–1 mm sample exhibited relatively large error). In this study, the physical model assumes that the Fabry–Perot effect of multiple reflections (i.e., $FP(\omega) = 1$) is ignored and only consider the first pulse. When the sample is thinner below 0.5mm, the THz pulse echoes are superimposed. For the thick sample, a number of multiple reflections are lower the thin sample because the optical path of the reflected wave inside the sample is long. This thing will lead to not clearly distinguishable in the time-domain data.

The parameters for the other polymers were similar to those reported in the literature. The minor differences between the measured and previously reported values may be due to differences in surface roughness resulting from the manufacturer's fabrication of the specimens used here.

4. Conclusion

THz-TDS is a relatively new measurement technology developed in recent years. Here, we present a rapid measurement method using a THz-TDS test system to evaluate various polymers based on their different polarities and compositional conditions. The data reported here are expected to be useful in the design of high-frequency electronics and optical devices. The THz spectra of nine common polymers were studied by THz-TDS. The THz frequency spectra for absorption and refractive index were obtained for each polymer. The results show that non-polar materials exhibit visible absorption characteristics and that the absorption spectra of different polymers differ significantly. We further presented an error analysis and explored practical applications of this measurement technique.

Through the debugging of the test system, the working parameters that are most suitable for the experimental testing were obtained. We further discussed the influence of water on the absorption of THz waves and, thus, on the extracted results. The experimental results show that the effects of moisture vary with the sample thickness in the band above 0.8 THz. In future studies, the measurement atmosphere will be filled with nitrogen until the air reaches 10–12% RH. Further, it was found that it is essential to measure the exact thickness of the sample in advance as the effect of thickness error on the refractive index and the absorption coefficient increases with the form of an exponential function with base e. This will provide experimental data and research basis for the application of THz-TDS technology for future practical analyses.

5. Future Work

Following this study, further spectral analysis of polymers should be carried out over a wider band to supplement the properties reported here for the range of 1–20 THz.

Acknowledgments

I would like to thank for my supervisor Prof PUN, Edwin Y B your support and guiding.

I would also like to express my heartfelt thanks to Dr. Chen, Bao Jie for his patient guidance, warm encouragement and helpful of this whole project.

References

[1] Peter H, Siegel. Terahertz Technology[J]. IEEE Transactions on microwave theory and techniques, 2002, 50(3): 910-920.

[2] Dragoman D, Dragoman M. Review terahertz fields and applications [J]. Progress in Quantum Electronics, 2004, 28(1): 1-66.

[3] M. Yin, S. Tang and M. Tong, "The application of terahertz spectroscopy to liquid petrochemicals detection: A review", Applied Spectroscopy Reviews, vol. 51, no. 5, pp. 379-396, 2016. Available: 10.1080/05704928.2016.1141291 [Accessed 10 April 2019].

[4] M. Godon, J. Carlier and A. Bauer, "Laboratory studies of water vapor absorption in the atmospheric window at 213 GHz", Journal of Quantitative Spectroscopy and Radiative Transfer, vol. 47, no. 4, pp. 275-285, 1992. Available: 10.1016/0022-4073(92)90146-u.

[5] Bour Petr. A cluster model of liquid water and its IR spectroscopic response[J]. Chem. Phys. Letter. 2002, 365(14): 82-88.

[6] Burda Kvetoslava, Bader K P, Schmid G H J. Anestimation of the size of the water cluster present at the cleavage site of the water splitting [J]. FEBS Letters, 2001, 491(15): 81-84.

[7] Zhao Lin. Study on formation mechanism of prethermodenaturation new peak of protein[J]. ACTA Biophysica Sinica, 1999, 15(11): 627-630.

[8] Martin van Exter, Ch. Fattinger, Grischkowsky. Terahertz time-domain spectroscopy of water vapor[J]. Optics Letters, 1989, 14(14): 1128-1130.

[9] R. Alan Cheville, D.Grischkowsky. Observation of pure rotation absorption spectra in the v2 band of hot H2O in flames[J]. Optics Letters, 1998, 23(12): 531-533.

[10] Takashi Arikawa, Kumiko Yamashita, Hikdeki Hirori. Complex dielectric constant of amino-acid solution revealed by THz time-domain attenuated total reflection technique[J]. OTST, 2005, 12(10): 11-33.

[11] Wei Shi and Yujie J. Ding. Direct measurement of resonant frequencies for H2O in the range of 0.2-4.2 THz by frequency-tuning monochromatic THz source[J]. CLEO, 2004, 23(14): 1-12.

[12] Y. Wang, et.al, “Restoration of terahertz signals distorted by atmospheric water vapor Absorption,” J. App. Phy. 105, 103105, 2009.

[13] Jin Y S, Kim G J, Jeon S G. Terahertz dielectric properties of polymers [J]. Journal of the Korean Physical Society, 2006, 49(2): 513-517.

[14] Fedulova EV, Nazarov MM, Angeluts AA, Kitai MS, Sokolov MI, and Shkurinov AP, Studying of dielectric properties of polymers in the terahertz frequency range. [J] Saratov Fall Meeting 2011: Optical Technologies in Biophysics and Medicine XIII, 2012.

[15] Naftaly M, Miles RE. Terahertz time-domain spectroscopy for material characterization[J] Proc. IEEE, 2007, 95(8): 1658-1665.

[16] Hejase J, Paladhi P, Chahal P. Corrections to terahertz characterization of dielectric substrates for component design and non-destructive evaluation of packages. IEEE Transactions on Components, Packaging and Manufacturing Technology. 2013, 3(2): 357-357.

[17] Chang T, Zhang X, Zhang X, Cui H. Accurate determination of dielectric permittivity of polymers from 75 GHz to 16 THz using both S-parameters and transmission spectroscopy. Applied Optics. 2017, 56 (12): 3287.

[18] Piesiewicz R, Jansen C, Wietzke S, Mittleman D, Koch M, Kürner T. Properties of building and plastic materials in the THz range. International Journal of Infrared and Millimeter Waves

[19] Tajvidi M, Ebrahimi G. Water uptake and mechanical characteristics of natural filler-polypropylene composites[J]. Journal of Applied Polymer Science, 2003, 88(4): 941-946.